Combined XANES and EXAFS analysis of Co^{2+}, Ni^{2+}, and Zn^{2+} aqueous solutions

P. D'Angelo*
Dipartimento di Chimica, Università di Roma "La Sapienza," Piazzale Aldo Moro 5, 00185 Rome, Italy and INFM, UdR Camerino, Italy

M. Benfatto
Laboratori Nazionali di Frascati-INFN, P.O. Box 13-00044, Frascati, Italy

S. Della Longa
Dipartimento di Medicina Sperimentale, Università L'Aquila, 67100 L'Aquila, Italy and INFM, UdR Roma "La Sapienza," Piazzale Aldo Moro 5, 00185 Rome, Italy

N. V. Pavel
Dipartimento di Chimica, Università di Roma "La Sapienza," Piazzale Aldo Moro 5, 00185 Rome, Italy
(Received 13 March 2002; revised manuscript received 19 June 2002; published 20 August 2002)

A combined x-ray-absorption near edge structure (XANES) and extended x-ray-absorption fine-structure (EXAFS) quantitative analysis of Co^{2+}, Ni^{2+}, and Zn^{2+} in water solutions based on fitting procedures of both low- and high-energy ranges has been carried out. The hydrogen contribution has been accounted for in both analyses and the effect of its inclusion on the structural parameters has been highlighted. The structural results obtained from the XANES and EXAFS analyses are in good agreement, confirming the validity of the application of the multiple-scattering theory in the low-energy range of the x-ray-absorption spectra. A systematic shortening of the ion-water first shell distance of about 0.03 Å is obtained from the XANES analyses, as compared to the EXAFS one. The origin of this systematic effect has been deeply investigated and it has been found to be due to the low-energy behavior of the real part of the Hedin-Lundqvist potential used in the calculations.

DOI: 10.1103/PhysRevB.66.064209 PACS number(s): 78.70.Dm, 71.20.Ps

I. INTRODUCTION

X-ray-absorption spectroscopy (XAS) is one of the most powerful methods to obtain structural and electronic information on the local environment of an excited atom. During the past ten years, much theoretical and computational efforts have led to the development of *ab initio* methods for XAS calculations in arbitrary systems. Over 50 eV above the rising edge an important approximation can be made which leads to the reduction of the many-body process in a photoelectron scattering in an effective potential. This allows a quantitative analysis of the extended x-ray-absorption fine-structure (EXAFS) region of the XAS spectra. The EXAFS technique has found many applications ranging from chemistry to molecular biology, including liquid and solid-state problems in condensed-matter physics.

The situation is different concerning the low-energy part of the x-ray-absorption cross section extending up to around 50 eV above the threshold, the so-called x-ray-absorption near-edge structure (XANES) region. This part is very sensitive to the structural details of the absorbing site and, in principle, an almost complete recovery of the three-dimensional structure can be achieved from the experimental data. However, the analysis of the low-energy region is much more difficult to perform as several non-negligible processes [many-body effects, multiple-scattering (MS) effects of any order, and so on] contribute to this part of the spectrum. The quantitative analysis of XANES requires an adequate treatment of the potential, a proper many-body theory, and the use of heavy time-consuming algorithms to calculate the absorption cross section in the framework of the full MS approach.[1,2] For this reason this technique has been so far used as a ''qualitative'' method and only recently attempts have been made to perform a quantitative analysis of the XANES experimental data in terms of a defined set of structural parameters. The possibility to gain structural information from the XANES spectra is extremely important for dilute and biological systems where the low S/N ratio of the experimental data hampers a reliable analysis of the EXAFS region.

Recently, a method has been proposed in the literature which performs a quantitative analysis of XANES.[3–5] In particular a new software procedure, named MXAN, has been developed and it has been successfully applied to the structural investigation of biological systems and ionic aqueous solutions.[3,4,6] This method is based on the comparison between the XANES experimental data and several theoretical calculations performed by varying selected structural parameters associated with a starting model. Starting from a putative geometrical configuration around the absorber atom the MXAN package is able to reach the best-fit conditions in a reasonable time by minimizing the square residual in the parameter space. The x-ray photoabsorption cross section is calculated using the full MS scheme in the framework of the muffin-tin (MT) approximation.

Even though the correctness of the MXAN method has been previously proved by investigating several test cases,[3,4] the aim of this work is to further validate this procedure and

to define its potentialities and limitations. To this end we carried out a comparison of the structural results obtained from the XANES and EXAFS analyses of Co^{2+}, Ni^{2+}, and Zn^{2+} aqueous solutions. These systems are an ideal test case as it is well established that the inner hydration shell of Co^{2+}, Ni^{2+}, and Zn^{2+} has an octahedral structure with six tightly bound water molecules. A detailed investigation of the hydration structure of these ions has been recently carried out combining EXAFS spectroscopy and molecular-dynamics (MD) simulations.[7] The EXAFS data analysis has been performed by means of the GNXAS package[8] whose reliability is well established. The ion-oxygen first shell structural parameters have been accurately determined and compared with previous experimental results. The ion-hydrogen interactions have been found to provide a detectable contribution to the EXAFS spectra of several aqueous and nonaqueous ionic solutions[9–11] and their inclusion has been proved to be important to perform a reliable data analysis. Moreover high quality data are available in a large energy range improving the accuracy of the EXAFS structural results.

The purpose of the present study is to assess the accuracy of the MXAN structural determination of simple systems involving ions of biological interest such as Co, Ni, and Zn. These results are essential to understand the new role that XANES can play in complementing the structural information obtained by EXAFS and in providing new insights into chemical and electronic structure.

II. METHODS

A. Experimental section

0.2 M Co^{2+}, Ni^{2+}, and Zn^{2+} aqueous solutions were obtained by dissolving the appropriate amount of $Zn(NO_3)_2$, $Ni(NO_3)_2$, and $Co(NO_3)_2$ in water, respectively. XAS spectra at the Co, Ni, and Zn *K* edges were recorded in transmission mode using the EMBL spectrometer at DESY.[12] Measurements were performed at room temperature with a Si(111) double-crystal monochromator and 50% harmonic rejection achieved by slightly detuning the two crystals from parallel alignment. For each sample three spectra were recorded and averaged after performing an absolute energy calibration.[13,14] The DORIS III storage ring was running at an energy of 4.4 GeV with positron currents between 70 and 40 mA. The solutions were kept in cells with Kapton film windows and Teflon spacers of 2 mm for Zn, and 1 mm for Co and Ni.

B. Theoretical details

The EXAFS investigation has been carried out using a method which refines ion-water radial distribution models obtained from MD simulations on the basis of the experimental data.[7] As previously mentioned the data analysis has been performed using the GNXAS set of programs.[8] A thorough description of this procedure and the structural results obtained for Co^{2+}, Ni^{2+}, and Zn^{2+} water solutions can be found in Ref. 7. It is worth noting that this was the first EXAFS investigation of 3*d* transition-metal ions in aqueous solution where the ion-H contribution has been taken into account. Phase shifts have been calculated using the muffin-tin approximation with MT radii of 0.2 and 0.9 Å, for hydrogen and oxygen, respectively, and 1.2 Å for cobalt, nickel, and zinc. The MT radius of the hydrogen atoms has been adjusted so as not to overestimate the signal from the scattering of the hydrogen atoms, which is expected to be weak. The hydrogen MT radius chosen corresponds to about 0.06 electrons for the integral of the charge density.

The XANES data analysis has been performed by a procedure, named MXAN, which is described in detail in Ref. 3. The x-ray-absorption cross section is calculated using the general MS scheme within the muffin-tin approximation for the shape of the potential. Twelve hydrogen atoms have been included as scatterer atoms in the calculations using the geometry and the orientation of a previous molecular-dynamics study[15] according to which the ion, oxygen, and two hydrogen atoms lie in one plane in a so-called ''dipole'' configuration. The exchange and correlation parts of the potential are determined on the basis of the local-density approximation of the self-energy of the excited photoelectron using an appropriate complex optical potential.[1] The real part of self-energy is calculated either by the X_α approximation or by using the Hedin-Lundqvist (HL) energy-dependent potential.[16] In the case of covalent molecular systems, to avoid over-damping at low energies due to the complex part of the HL potential,[2,17] the MXAN method can account for all inelastic processes by convolution with a broadening Lorentzian function having an energy-dependent width of the form $\Gamma(E)=\Gamma_c+\Gamma_{mfp}(E)$. The constant part Γ_c accounts for both the core-hole lifetime and the experimental resolution, while the energy-dependent term represents all the intrinsic and extrinsic inelastic processes. The $\Gamma_{mfp}(E)$ function is zero below an energy onset E_s (which, in extended systems, corresponds to the plasmon excitation energy) and starts increasing from a given value *A*, following the universal functional form of the mean free path in solids.[18] Both the onset energy E_s and the jump *A* are introduced in the $\Gamma_{mfp}(E)$ function via an arctangent functional form to avoid discontinuities. Their numerical values are derived at each step of computation on the basis of a Monte Carlo search, similarly to the procedure used in optimizations by simulated annealing.[19] This type of approach can be justified on the basis of a multichannel MS theory.[20] In the sudden limit, the net absorption is given by a sum over all the possible excited states of the $(N\text{-}1)$-electron system.[2,20,21] By assuming that the channels coming from the excitation of the N-1 electrons are near in energy, the total absorption is given by a convolution of the one-particle spectrum, calculated with the full-relaxed potential, with a spectral function representing the weight of the other excited states. Hence the total XAS cross section can be written as

$$\mu=\sum_n (\mu_n)_{\Delta E\to 0}\to \int \mu(\omega-\omega')A(\omega')d\omega', \qquad (1)$$

where the ''ansatz'' is made that the spectral function $A(\omega')$ is well approximated by a Lorentzian function with the energy-dependent width $\Gamma(E)$ previously defined. Obvi-

ously, when contributions from one or more of these excited states become relevant, they must be considered explicitly in the calculations. It is also possible to demonstrate that this convolution procedure is equivalent to a calculation performed with a potential containing an appropriate complex part derived by reducing a multichannel process to a single-channel one.[22] Therefore the $\Gamma(E)$ function is characterized by parameters which have a clear physical meaning and they are not free to assume any value, but are varied in a well-defined interval.

The potential has been calculated using the same MT radii of the EXAFS analysis for the oxygen, hydrogen, cobalt, and nickel atoms. A different choice has been made for zinc (1.35 Å) due to the bigger ionic radius of Zn^{2+} as compared to the other two ions. It is important to stress that the potential is calculated at each step of the fitting procedure for each structural configuration. The importance of this procedure has been assessed in a previous investigation of Ni^{2+} in water solution where it has been shown that small changes in the structure can produce detectable differences in the potential, especially in the low-energy range of the spectra.[3] This is particularly important when an accurate analysis of the XANES has to be performed.

III. RESULTS

In the first step of the XANES analysis the experimental data have been fitted starting from a distorted octahedral configuration of the oxygen atoms around the three ions. A real HL potential has been used in the calculations and inelastic losses have been accounted for by a convolution with a Lorentzian function, as previously described. The best-fit analyses of the Co^{2+}, Ni^{2+}, and Zn^{2+} water solution XANES spectra are shown in the upper, middle, and lower panels of Fig. 1, respectively. Overall, the fitted XANES spectra match the experimental data quite well and only small discrepancies can be observed in the first 10 eV from the edge for Co^{2+} and Ni^{2+}, while more relevant differences are present in the case of Zn^{2+}. This mismatch is probably due to inaccuracies of the potential associated with the MT approximation, which are more relevant in the very low-energy part of the spectrum.[23] From the fitting procedure a regular octahedral coordination of the water molecules around the ions has been found, and the corresponding first shell distances are listed in Table I, together with the EXAFS structural results obtained from the GNXAS analysis.[7] It is important to outline that all the XANES minimizations have lead to a regular octahedral hydration complex, even when two or three different coordination distances were used in the fitting procedure. Nevertheless, due to the geometrical symmetry of the cluster, a strong correlation among the structural parameters has been found when more than one ion-oxygen distance was minimized. This hampered a reliable determination of the statistical errors associated with the structural parameters and therefore, in Table I, we report only the results associated with the single distance best-fit analysis.

The Γ_c values obtained from the fitting procedures are also listed in Table I. While for Co^{2+} and Ni^{2+} these parameters are in reasonable agreement with the sum of the core-hole width (1.33 and 1.44 eV for Co and Ni, respectively[24]) and the experimental resolution, the Γ_c value for Zn^{2+} is too large. This is most probably due to the discrepancy between theory and experiment in the low-energy range where the effect of this part of the damping is more important.

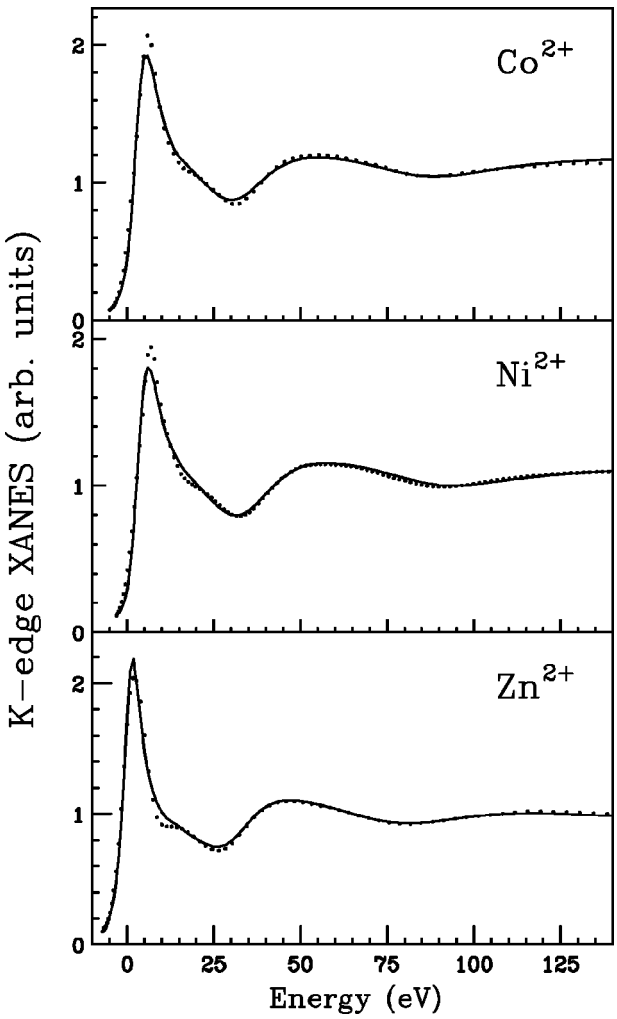

FIG. 1. Comparison between the best-fit theoretical XANES spectra (solid lines) of Co^{2+}, Ni^{2+}, and Zn^{2+} water solutions (upper, middle, and lower panels, respectively) and the raw experimental data (dotted lines).

In the second step of the analysis, proof of the validity of the phenomenological approach used by the MXAN procedure to account for extrinsic inelastic losses was obtained by performing additional calculations with complex HL potentials.

TABLE I. XANES refined parameters for Co^{2+}, Ni^{2+}, and Zn^{2+} water solutions and comparison with the EXAFS structural results.

	R(Å)	Γ_c	R(Å)[a]
Co	2.06(0.03)	2.07	2.092(0.002)
Ni	2.03(0.03)	1.70	2.072(0.002)
Zn	2.06(0.02)	3.14	2.078(0.002)

[a]From Ref. 7.

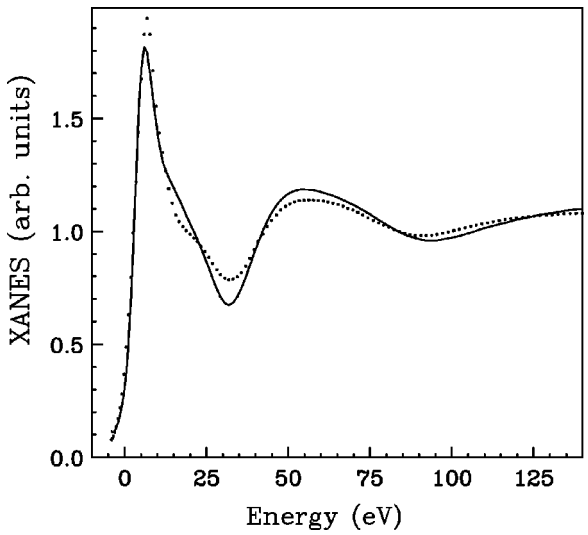

FIG. 2. Comparison between the XANES experimental spectrum (dotted line) of the Ni^{2+} aqueous solution and best-fit theoretical curve (solid line) calculated with the Hedin-Lundqvist complex potential.

The contribution of the core-hole and experimental resolution has been included by convolution with a broadening Lorentzian function having the same width reported in Table I for the Ni^{2+} ion. The results of this analysis for the Ni^{2+} solution are shown in Fig. 2, where the theoretical best-fit curve is compared to the experimental spectrum. The agreement between theory and experiment is quite poor in the low-energy region up to about 50 eV and it improves as the energy increases. Nevertheless, the geometrical structure which has been obtained from this minimization corresponds to an octahedron with a Ni-O distance of 2.04 ± 0.03 Å, which is the same results, within the reported errors, of the previous analysis. It is noticeable that a correct structure is recovered in spite of the low-energy disagreement between the experimental and theoretical curves.

In order to gain a deeper insight into the effect of the potential details on both the quality of the fits and the accuracy of the structural determination, we report in Fig. 3 the best-fit results for the Zn^{2+} ion performed with a different MT radius and with the X_α potential. In the upper panel we show the comparison between the experimental data and theoretical best-fit calculations performed with a Zn MT radius of 1.2 Å, which is the same value used for the other two ions. From the minimization procedure a Zn-O distance of 2.05 ± 0.05 Å has been obtained with an error function $R_{sq} = 4.8$,[3,6] which is twice as large as the one obtained from the previous analysis. In the lower panel of Fig. 3 the best-fit analysis of the calculations performed with the X_α potential is reported. In this case a shorter Zn-O distance value has been obtained (2.04 ± 0.04 Å) while the agreement between the theoretical and experimental spectra is of the same quality as the one reported in Fig. 1 ($R_{sq} = 2.9$). This finding demonstrates that XANES is essentially dominated by the geometrical arrangement of atoms around the photoabsorber, while it is less sensitive to the potential details. Further proof of this theoretical assessment has been obtained by comparing the experimental data with a theoretical calculation performed with different geometries of the ion-O complexes. In particular in the upper panel of Fig. 4 we show the comparison between the experimental data and the theoretical curve associated with a regular octahedron with a Zn-O distance of 2.16 Å. Relevant discrepancies between the two spectra are present in the whole energy range giving $R_{sq} = 6.1$. The effect of a Jahn-Teller distortion has been accounted for by performing a calculation with a Zn-O axial distance of 2.36 Å, keeping the in-plane distance equal to 2.06 Å. The results of this analysis are shown in the lower panel of Fig. 4. Also in this case discrepancies are present in the whole energy range and a poorer agreement between theory and experiment has been obtained as compared to Fig. 1 ($R_{sq} = 4.2$).

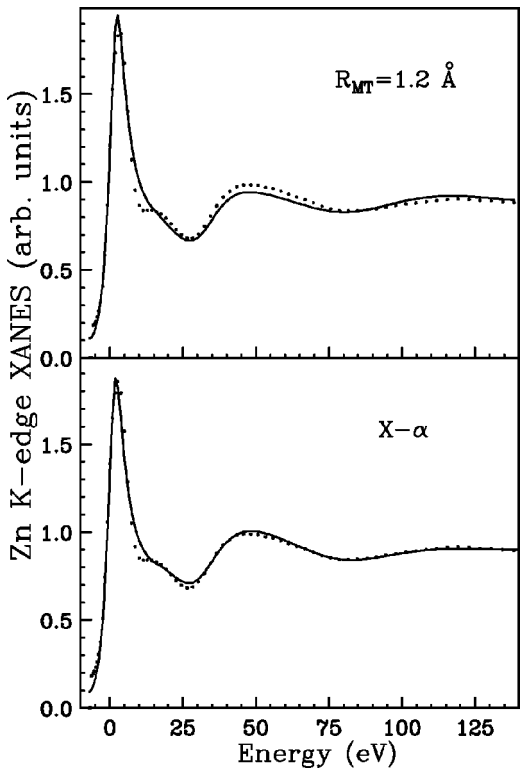

FIG. 3. Comparison between the XANES experimental spectrum (dotted lines) of the Zn^{2+} aqueous solution and best-fit theoretical curve (solid lines) calculated with a different choice of the Zn MT radius (upper panel) and with the X_α potential (lower panel).

The outstanding result of this study concerns the systematic shortening of the XANES structural determinations of about 0.03 Å as compared to the EXAFS ones (see Table I). It is interesting to outline that the Zn^{2+} first hydration shell parameters obtained by the present GNXAS analysis are equal, within the reported errors, to those determined by the most recent EXAFS investigation performed by the FEFF program.[25] In order to understand the origin of this discrepancy one has to make some general considerations about the theoretical framework of the MXAN method. Due to the shape of the spectra, the XANES minimizations are more sensitive to the low-energy region, which is dominated by a strong resonance after the rising edge. At the same time in this part

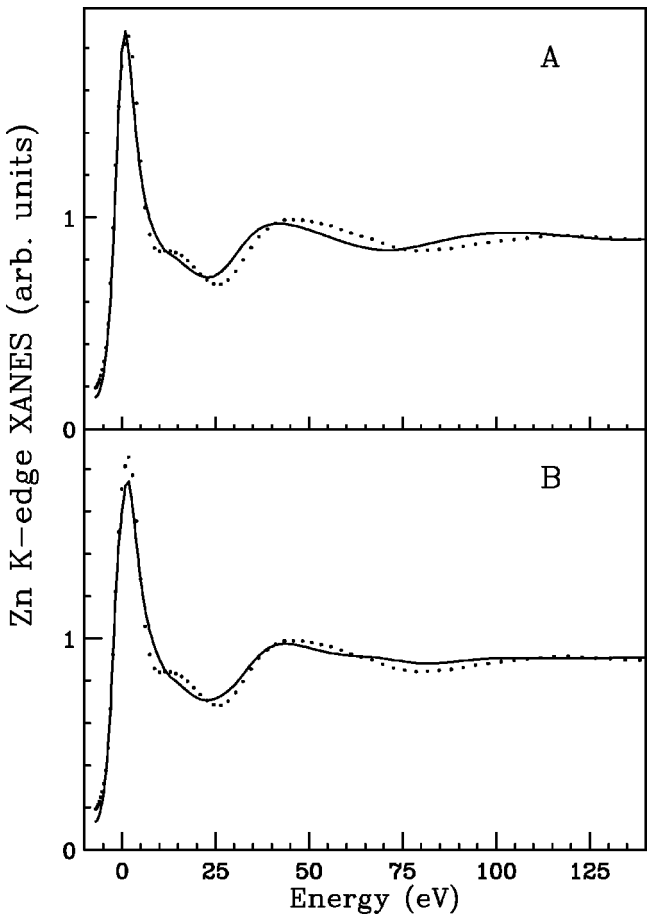

FIG. 4. Comparison between the XANES experimental spectrum (dotted lines) of the Zn^{2+} aqueous solution and two calculations (solid lines) performed with different Zn-O geometries. (a) A regular octahedral geometry with a Zn-O distance of 2.16 Å has been used. (b) A Jahn-Teller distorted geometry with a Zn-O in-plane distance of 2.06 Å and an axial distance of 2.36 Å has been considered.

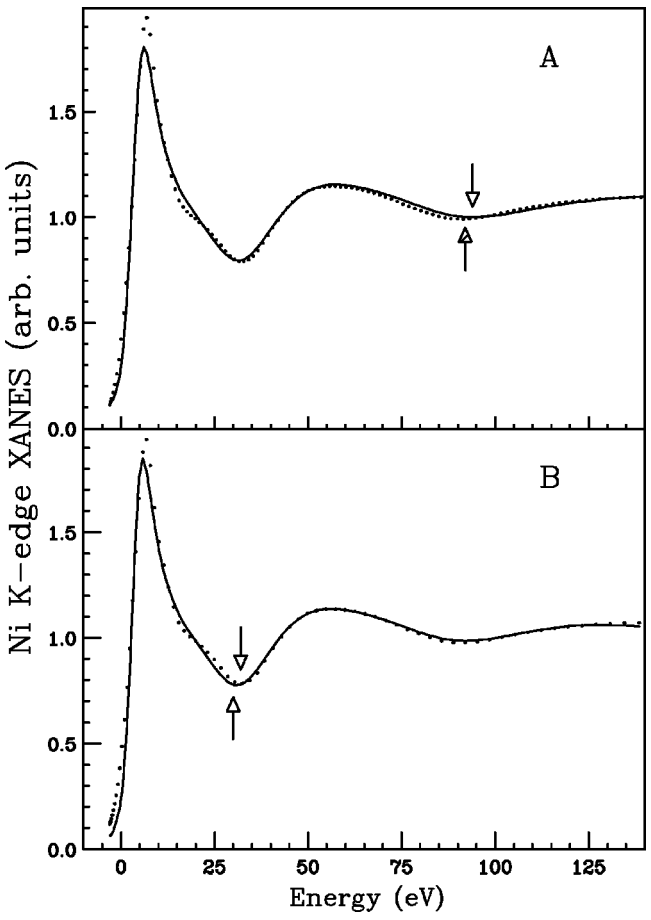

FIG. 5. Comparison between the XANES experimental spectrum (dotted lines) of the Ni^{2+} aqueous solution and best-fit theoretical curves (solid lines) obtained with no statistical weight (a) and with statistical weight (b).

of the spectrum the real part of the HL potential is essentially energy independent, resembling the behavior of the X_α potential. It is well known that use of the X_α potential results in a compressed energy scale spectrum as compared to the experimental data[2,26] and a shortening of the first shell distances is necessary to realign the theoretical energy scale to the experimental one. Therefore, the systematic shortening of the coordination distance obtained from the MXAN minimizations is most probably due to the low-energy behavior of the real part of the HL potential.

In order to verify this hypothesis we have carried out a fitting procedure using an arctangent weight function and all details on this method can be found in Ref. 3. In this way it is possible to weight more the high-energy region of the absorption spectrum, which is less affected by inaccuracies of the theory. The results of this analysis are shown in Fig. 5 for the Ni^{2+} aqueous solution. In the upper panel of this figure we report the comparison between the best-fit curve with no statistical weight and the experimental data. Note that the agreement between the two spectra is not perfect in the minimum-energy region around 90 eV. The lower panel of Fig. 5 shows the results of the minimization performed with the weight function. As expected, when a statistical weight is used in the fitting procedure, the agreement between the calculated and experimental spectra improves in the high-energy part, while more evident discrepancies can be observed in the first minimum region at about 30 eV. At the same time a longer Ni-O first shell distance (2.05 ± 0.02 Å) has been obtained from the latter minimization as compared to the previous analysis. This finding further enforces the idea that the differences between the XANES and EXAFS structural determinations stem from the low-energy behavior of the real part of the HL potential and the results of the two techniques get closer when the XANES analysis is carried out weighting more the high-energy region of the spectrum.

To definitely prove this hypothesis we have carried out a new EXAFS analysis of the Co^{2+}, Ni^{2+}, and Zn^{2+} aqueous solutions using the X_α potential in the phase-shift calculations. The minimizations have been performed using the same strategy described in Ref. 7. The results of these fitting procedures are shown in Fig. 6, where the total theoretical signals, including the ion-oxygen and ion-hydrogen first shell and the MS contributions, are compared with the EXAFS experimental spectra. In all cases the agreement be-

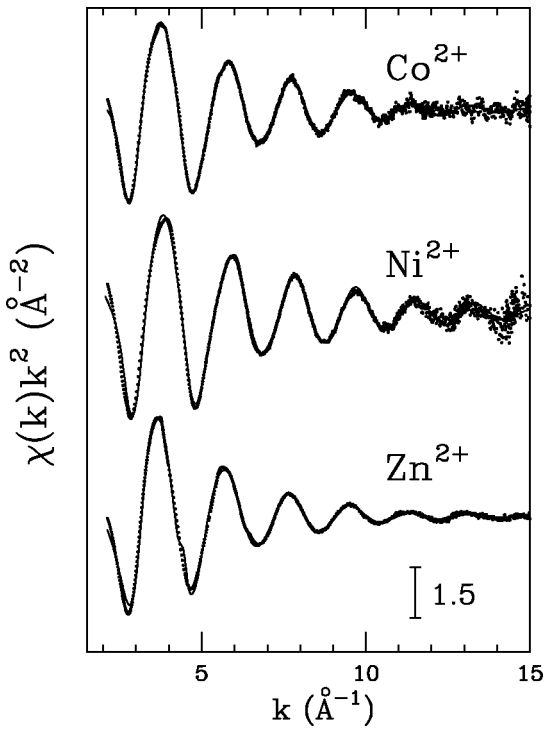

FIG. 6. Comparisons between the EXAFS experimental spectra (dotted lines) of Co^{2+}, Ni^{2+}, and Zn^{2+} in water solutions and theoretical signals (solid lines) calculated with the X_α potential.

tween the experimental and theoretical signals in the *k* region below 3 $Å^{-1}$ is not as good as that obtained with the HL potential (see Fig. 2 of Ref. 7). The ion-oxygen first shell distances determined from the minimizations are 2.070 ± 0.006, 2.050 ± 0.006, and 2.060 ± 0.005 Å, for Co^{2+}, Ni^{2+}, and Zn^{2+}, respectively, while all the other structural and nonstructural parameters were found equal to those obtained using the HL potential (see Table 3 of Ref. 7). It is noticeable that the use of the X_α potential in the EXAFS calculation leads to the same structural parameters, within the error bar, obtained by the MXAN method.

A last remark we would like to make concerns the effect of the inclusion of the hydrogen atoms in the XANES investigation. In a previous MXAN analysis of a Ni^{2+} aqueous solution the hydrogen atoms were not included in the calculations and the Ni-O first shell distance obtained was 2.00 ± 0.04 Å with a Γ_c value of about 2.6 eV.[3] Note that the exclusion of the hydrogen atoms affects both the ion-oxygen distance and the width of the calculated shape resonance. On the contrary it has been shown that even if the hydrogen atoms provide a detectable contribution to the EXAFS spectra of 3*d* metal ions in aqueous solution, their exclusion does not significantly affect the accuracy of the ion-oxygen first shell structural parameters.[7] From these results it is clear that the XANES technique is very sensitive to the presence of the hydrogen atoms and their inclusion is essential to perform a reliable determination of the structural parameters.

IV. CONCLUSIONS

The development of the MXAN code now makes possible a general treatment of XAS, encompassing both EXAFS and XANES. A quantitative analysis based on the fitting procedure of the whole XAS spectra, including the threshold region, has been carried out for Co^{2+}, Ni^{2+}, and Zn^{2+} ions in water solution. Comparison of the ion-water first shell structural results allowed the accuracy of the MXAN method to be assessed. The MXAN method has been proven to provide reliable structural results confirming the validity of the application of the full MS scheme in the framework of the MT approximation, in the case of 3*d* metal ions in aqueous solutions. A systematic shortening of the ion-oxygen distance obtained from the XANES data analysis has been observed, as compared to the EXAFS determination. The origin of this effect has been deeply investigated and it has been found to be due to the low-energy behavior of the real part of the HL potential. The hydrogen atoms have been accounted for in the MXAN analysis and their inclusion has been found to be essential to perform a reliable determination of the ion-oxygen first shell parameters. The results of the present investigation represent a step forward in understanding the role that the XANES technique can play in providing quantitative structural information on chemical systems.

ACKNOWLEDGMENTS

We thank the European Union for support of the work at EMBL Hamburg through the HCMP Access to a Large Installation Project, Contract No. HPRI-CT-1999-00017, and the CASPUR computational center for providing the computer architectures used in this work. Paola D'Angelo was supported by an institutional EU fellowship, Contract No. ERBCHBGCT930485. This work was sponsored by the Italian National Research Council and by the Italian Ministry for the University and the Scientific and Technological Research (MURST).

*Email address: p.dangelo@caspur.it

[1] T.A. Tyson, K.O. Hodgson, C.R. Natoli, and M. Benfatto, Phys. Rev. B **46**, 5997 (1992).
[2] J.J. Rehr and R.C. Albers, Rev. Mod. Phys. **72**, 621 (2000).
[3] M. Benfatto and S. Della Longa, J. Synchrotron Radiat. **8**, 1087 (2001).
[4] S. Della Longa, A. Arcovito, M. Girasole, J.L. Hazemann, and M. Benfatto, Phys. Rev. Lett. **87**, 155501 (2001).
[5] M. Benfatto, S. Della Longa, and C. R. Natoli (unpublished).
[6] M. Benfatto, P. D'Angelo, S. Della Longa, and N.V. Pavel, Phys. Rev. B **65**, 174205 (2002).
[7] P. D'Angelo, V. Barone, G. Chillemi, N. Sanna, W. Meyer-Klaucke, and N.V. Pavel, J. Am. Chem. Soc. **124**, 1958 (2002).
[8] A. Filipponi and A. Di Cicco, Phys. Rev. B **52**, 15 135 (1995).
[9] D. Roccatano, H.J. Berendsen, and P. D'Angelo, J. Chem. Phys. **108**, 9487 (1998).
[10] P. D'Angelo, N.V. Pavel, D. Roccatano, and H.-F. Nolting, Phys. Rev. B **54**, 12 129 (1996).
[11] P. D'Angelo, A. Di Nola, M. Mangoni, and N.V. Pavel, J. Chem. Phys. **104**, 1779 (1996).

[12] C. Hermes, E. Gilberg, and M.H. Koch, Nucl. Instrum. Methods Phys. Res. A **222**, 207 (1984).
[13] R.F. Pettifer and C. Hermes, J. Phys. Colloq. **47**, C8-127 (1986).
[14] R.F. Pettifer and C. Hermes, J. Appl. Crystallogr. **18**, 404 (1985).
[15] G. Chillemi, P. D'Angelo, N.V. Pavel, N. Sanna, and V. Barone, J. Am. Chem. Soc. **124**, 1968 (2002).
[16] L. Hedin and S. Lundqvist, Solid State Phys. **23**, 1 (1969).
[17] M. Benfatto, J.A. Solera, J. Chaboy, M.G. Proietti, and J. García, Phys. Rev. B **56**, 2447 (1997).
[18] J.E. Muller, O. Jepsen, and J.W. Wilkins, Solid State Commun. **42**, 365 (1982).
[19] S. Kirkpatrick, C.D. Gelatt, Jr., and M.P. Vecchi, Science **220**, 671 (1983).
[20] C.R. Natoli, M. Benfatto, C. Brouder, M.F. Ruiz López, and D.L. Foulis, Phys. Rev. B **42**, 1944 (1990).
[21] S.H. Chou, J.J. Rehr, E.A. Stern, and E.R. Davidson, Phys. Rev. B **35**, 2604 (1987).
[22] C. R. Natoli, M. Benfatto, S. Della Longa, and K. Hatada (unpublished).
[23] Y. Joly, Phys. Rev. B **63**, 125120 (2001).
[24] M.O. Krause and J.H. Oliver, J. Phys. Chem. Ref. Data **8**, 329 (1979).
[25] A. Kuzmin, S. Obst, and J. Purans, J. Phys.: Condens. Matter **97**, 10 065 (1997).
[26] M. Benfatto, C.R. Natoli, A. Bianconi, J. García, A. Marcelli, M. Fanfoni, and I. Davoli, Phys. Rev. B **34**, 5774 (1986).